

Formation of Large Voids in the Amorphous Phase-Change Memory $\text{Ge}_2\text{Sb}_2\text{Te}_5$ Alloy

Zhimei Sun,^{1,*} Jian Zhou,¹ Andreas Blomqvist,² Börje Johansson,² and Rajeev Ahuja²

¹College of Materials, Xiamen University, 361005 Xiamen, China

²Department of Physics and Materials Science, Uppsala University, Box 530, 75121 Uppsala, Sweden

(Received 23 June 2008; published 19 February 2009)

On the basis of *ab initio* molecular dynamics simulations, large voids mainly surrounded by Te atoms are observed in molten and amorphous $\text{Ge}_2\text{Sb}_2\text{Te}_5$, which is due to the clustering of two- and threefold coordinated Te atoms. Furthermore, pressure shows a significant effect on the clustering of the under coordinated Te atoms and hence the formation of large voids. The present results demonstrate that both vacancies and Te play an important role in the fast reversible phase transition process.

DOI: 10.1103/PhysRevLett.102.075504

PACS numbers: 61.43.Dg, 61.43.Bn, 64.60.Cn, 71.15.Pd

One of the most important technological advances in the past decade is optical or electrical data storage [1–6], owing to the memory switch based on the pronounced optical or electrical contrast between the amorphous and crystalline states of multicomponent chalcogenides [7]. The data storage is achieved by the extremely fast and reversible phase transition between the metastable cubic (rocksalt structure) and amorphous states of Ge-Sb-Te alloys, among which $\text{Ge}_2\text{Sb}_2\text{Te}_5$ (GST) exhibits the best performance and is considered as the most promising candidate for phase-change random access memory (PCRAM) applications. The atomic arrangement in crystalline and amorphous GST is a hot topic to understand the mechanism of the fast reversible phase transition [8–14]. GST contains 20% vacancies in one sublattice of its rock-salt structure. Despite many fundamental works on the GST alloys, the behavior of vacancies has not been fully understood. Wuttig *et al.* have performed static *ab initio* calculations to understand the role of vacancies in cubic Ge-Sb-Te [6]. In our previous work, we proposed ordered arrangement of vacancies in cubic (*c*)-GST on the basis of *ab initio* calculations [14]. However, the arrangement of vacancies in amorphous (*a*)-GST remains unclear and no work on this topic has been reported so far.

In amorphous systems, the most obvious choice to identify vacancies or interstitials is to consider the local atomic structure and find the features that can be associated with vacancies or interstitials. In this Letter, we carried out *ab initio* molecular dynamics simulations to study the atomic arrangement in *a*-GST to understand the behavior of vacancies.

Our *ab initio* molecular dynamics simulations (AIMD) and static *ab initio* calculations were carried out using the VASP code [15]. Calculation parameters for the AIMD simulations and constructions of the initial configuration have been given in our previous work [14,16]. To investigate the effect of pressure, two densities have been used in this work, one is an experimental density of 0.0297 atoms/Å³ [17] for *a*-GST, the other is 0.0348 atoms/Å³ of a theoretical density for *c*-GST ob-

tained from our *ab initio* calculations at 0 K. For the melt and quench process, the supercells of 243 atoms plus 27 vacancy positions were melted and thermalized at 3000 K for 3 ps, wherein the temperature was controlled using the algorithm of Nosé [18]. Then the liquid is gradually quenched down to 300 K by a quenching rate of 6.6 K ps⁻¹ between a series of temperatures (for example, between 1000 and 900 K) and followed by an isothermal period of another 3 ps at these temperatures. The structural results presented in this Letter are derived from the configurations collected during the 3 ps simulations at 300 K.

One of the most interesting findings in the present work is that a large void mainly surrounded by Te aside from tiny cavities are observed in both molten and amorphous GST with a low density ($d_1 = 0.0297$ atom/Å³, denoted as *a1*-GST) at temperatures below its melting point (~900 K), while it is not observed in *a*-GST of the high density ($d_2 = 0.0348$ atom/Å³, denoted as *a2*-GST). Figures 1(a) and 1(b) show snapshot structures for *a1*-GST and *a2*-GST at 300 K, respectively, from which a large void is clearly seen in *a1*-GST as illustrated by “*v*” but it is not observed in *a2*-GST. To investigate the effect of cooling rate on the behavior of vacancies and also to completely rule out the memory of its original structure, the amorphous structure snapshot at 300 K is reheated to 5000 K and after being thermalized for 3 ps, it was quenched down to 300 K by a constant cooling rate of 50 times of the above one. Once again, a large void mainly surrounded by Te is clearly obvious in *a1*-GST marked as “*v*” in Fig. 1(c). The nominal pressures in *a1*-GST and *a2*-GST at 300 K were calculated to be ~1.2 and ~26 kbar, respectively. The results demonstrate significant effects of pressure on the formation of voids. A further analysis on *a1*-GST shows that those Te atoms surrounding the voids are mainly twofold and threefold coordinated. Recall that the 20% vacancies in the sublattice of *c*-GST are around Te atoms [14], the present results indicate that those defective Te atoms tend to cluster during quenching as the nominal pressure on molten GST is close to the atmospheric pressure. The driving force for the void for-

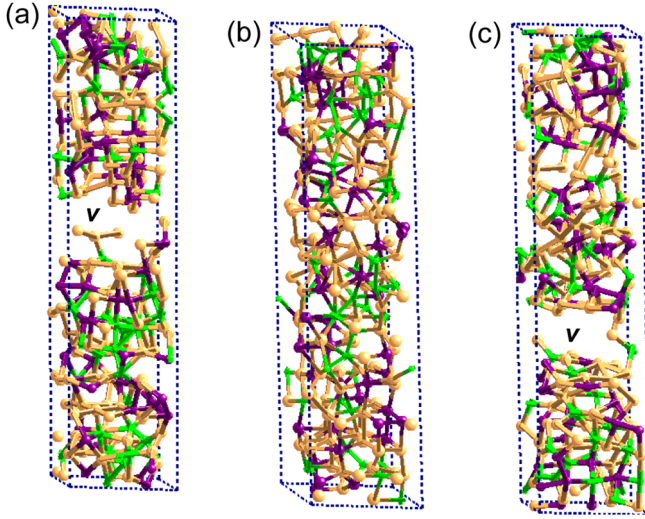


FIG. 1 (color online). Snapshot structures of a -GST at 300 K. (a) $a1$ -GST with a cooling rate of 6.6 K/ps, (b) $a2$ -GST, (c) $a1$ -GST with a cooling rate of 333 K/ps. Herein the large light atoms represent Te, middle dark atoms represent Sb and small light gray atoms represent Ge.

mation is the reduction of the total energy because the calculated cohesive energy difference between $a1$ -GST and its cubic structure at 0 K is ~ 0.10 eV/atom.

Figures 2(a) and 2(b) show the fractional distribution of coordination numbers (CNs) for Ge, Sb and Te in $a1$ -GST and $a2$ -GST, respectively. For Ge, fivefold and sixfold coordinations dominate in $a1$ -GST, while sixfold coordination dominates in $a2$ -GST. For Sb, sixfold coordination is dominated in both $a1$ -GST and $a2$ -GST. For Te, threefold and fourfold predominate in $a1$ -GST, while fourfold and fivefold predominate in $a2$ -GST. The results demonstrate significant effect of pressure on the distribution of CNs in a -GST, especially for Te. Furthermore, there are

$\sim 8\%$ twofold and $\sim 30\%$ threefold coordinated Te in $a1$ -GST, while the twofold coordinated Te is negligible and there is only $\sim 10\%$ threefold coordinated Te in $a2$ -GST. The under coordinated Te atoms in $a1$ -GST should have a significant amount of vacancies around them. As those Te atoms agglomerate, a large void will form as seen in Figs. 1(a) and 1(c), which is consistent with the above analysis. Therefore, the origin of the formation of large voids in molten $a1$ -GST is due to the under coordinated Te atoms.

Although the vacancy behaves differently in the two-density a -GST, the local atomic arrangements of which are quite similar and both resembles that of its cubic form as characterized by the bond angle distributions and pair distribution functions. Table I lists the CNs for each element in a -GST which are estimated by integrating the first peaks of the corresponding pair distribution functions. It is noted that the total CNs for Ge, Sb, and Te atoms suggests a mixture of multifold coordinated systems in a -GST which is consistent with that of a -GeSb₂Te₄ [12,16,19]. The numbers of heteropolar ($Z_{\text{Te-Ge}}$, $Z_{\text{Te-Sb}}$) and homopolar bonds ($Z_{\text{Ge-Ge}}$, $Z_{\text{Sb-Sb}}$ and $Z_{\text{Te-Te}}$) in $a2$ -GST are higher than that in $a1$ -GST and the total CNs of $a2$ -GST is either higher or closer to that of its cubic form, suggesting significant effects of pressure on the chemical-short-range order (CSRO) in a -GST. To quantify the chemical ordering, we used the normalized CSRO parameter as given in [20]. For Ge and Sb in a -GST, the parameters can be calculated by the following equation, where the subscript $x = \text{Ge}$ or Sb.

$$\alpha_x = \frac{1 - Z_{x-\text{Te}}/[c_{\text{Te}}(c_x Z_{\text{Te}} + c_{\text{Te}} Z_x)]}{1 - Z_x/[c_{\text{Te}}(c_x Z_{\text{Te}} + c_{\text{Te}} Z_x)]}. \quad (1)$$

For Te, since it is surrounded by Ge and Sb as the first nearest neighbors in c -GST, the CSRO parameter is calculated using Eq. (2):

$$\alpha_{\text{Te}} = \frac{1 - (Z_{\text{Te-Ge}} + Z_{\text{Te-Sb}})/\{(c_{\text{Ge}} + c_{\text{Sb}})[Z_{\text{Te}}(c_{\text{Ge}} + c_{\text{Sb}}) + c_{\text{Te}}(Z_{\text{Ge}} + Z_{\text{Sb}})]\}}{1 - Z_x/\{(c_{\text{Ge}} + c_{\text{Sb}})[Z_{\text{Te}}(c_{\text{Ge}} + c_{\text{Sb}}) + c_{\text{Te}}(Z_{\text{Ge}} + Z_{\text{Sb}})]\}}. \quad (2)$$

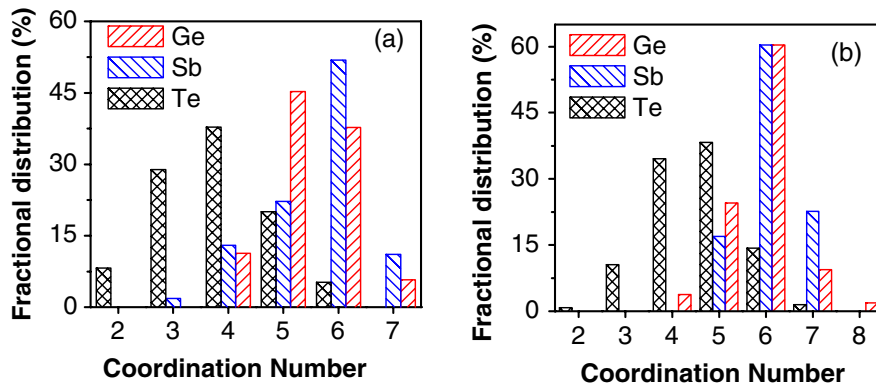


FIG. 2 (color online). Distribution of coordination numbers for Ge, Sb, and Te atoms in $a1$ -GST (a) and (b) $a2$ -GST at 300 K.

TABLE I. The estimated average coordination numbers (Z) for various pairs of atoms in amorphous and crystalline GST, where d_1 , d_2 refer to $a1$ -GST and $a2$ -GST, respectively, and Cry refers to rocksalt structured GST. The cutoff radii to integrate Z are the first minimums in the corresponding pair distribution functions.

	Z of Ge				Z of Sb				Z of Te			
	Z_{Ge-Ge}	Z_{Ge-Sb}	Z_{Ge-Te}	Z_{Ge}	Z_{Sb-Ge}	Z_{Sb-Sb}	Z_{Sb-Te}	Z_{Sb}	Z_{Te-Ge}	Z_{Te-Sb}	Z_{Te-Te}	Z_{Te}
$d1$	0.68	0.72	3.75	5.25	0.76	0.82	4.09	5.67	1.56	1.65	0.77	3.98
$d2$	0.86	0.90	3.96	5.72	0.92	1.00	4.33	6.25	1.60	1.72	1.14	4.46
$Cry.$	0	0	6.0	6.0	0	0	6.0	6.0	2.4	2.4	0	4.8

Herein $c_{Ge} = c_{Sb} = 0.2$ and $c_{Te} = 0.5$ are concentrations of Ge, Sb, and Te in c -GST, and Z represents values of coordination numbers in a -GST which are given in Table I. The value of α ranges from -1 (a phase separation) to 0 (a random mixture) and to 1 (a complete chemical ordering). For $a1$ -GST, we obtained $\alpha_{Ge} = 0.58$, $\alpha_{Sb} = 0.59$ and $\alpha_{Te} = 0.34$, and for $a2$ -GST, we got $\alpha_{Ge} = 0.54$, $\alpha_{Sb} = 0.55$ and $\alpha_{Te} = 0.16$. The results mean that the environment remains partly ordered especially around Ge and Sb atoms in a -GST. Furthermore, pressure shows a negligible effect on the CSRO of Ge and Sb, but a significant effect on that of Te. As the density of a -GST reduces by 17.2%, α_{Te} reduces by 52.9%. The absence of large voids in $a2$ -GST may partly be attributed to the relative lower CSRO around Te.

Figures 3(a) and 3(b) show bond angle distributions (BAD) around Ge, Sb, and Te in $a1$ -GST and $a2$ -GST, respectively. Around Ge, Sb, and Te, sharp peaks centering at $\sim 97^\circ$, $\sim 90^\circ$, and $\sim 89^\circ$ are observed in $a1$ -GST, respectively, while those at $\sim 92^\circ$, $\sim 89^\circ$, and $\sim 88^\circ$ are observed in $a2$ -GST, respectively. The results demonstrate that the configuration around the three species resembles that of the cubic form. In addition, the small broad peaks at $\sim 160^\circ$ indicate that the octahedrally coordinated a -GST is distorted. Furthermore, the angle distribution of various pairs of bonds with respect to the $[111]$ crystallographic direction shown in Fig. 4 gives more information. As seen in Figs. 4(a) and 4(c), the Te-Ge, Te-Sb, and Te-Te bonds

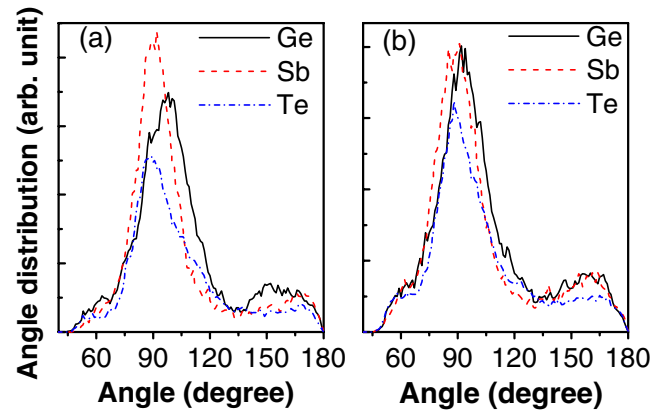


FIG. 3 (color online). Bond angle distributions calculated around Ge, Sb, and Te atoms in (a) $a1$ -GST and (b) $a2$ -GST.

are strongly correlated shown by the sharp peaks centering at $\sim 90^\circ$ for both a -GST phases. Compared with the vertical line existed in c -GST, the arrangement of the Te-Te bonds in a -GST resembles that in its cubic form. The arrangement of the Sb-Sb and Ge-Ge bonds also resembles that in its cubic form as seen by the peaks centering at $\sim 90^\circ$ in the angle distributions in Figs. 4(b) and 4(d) for $a1$ -GST $a2$ -GST, respectively. In addition, the Ge-Sb bond is also correlated and its peak position shifts from $\sim 94^\circ$ in $a1$ -GST to $\sim 100^\circ$ in $a2$ -GST. The features in Fig. 4 and the CSRO analysis above demonstrate a picture that the

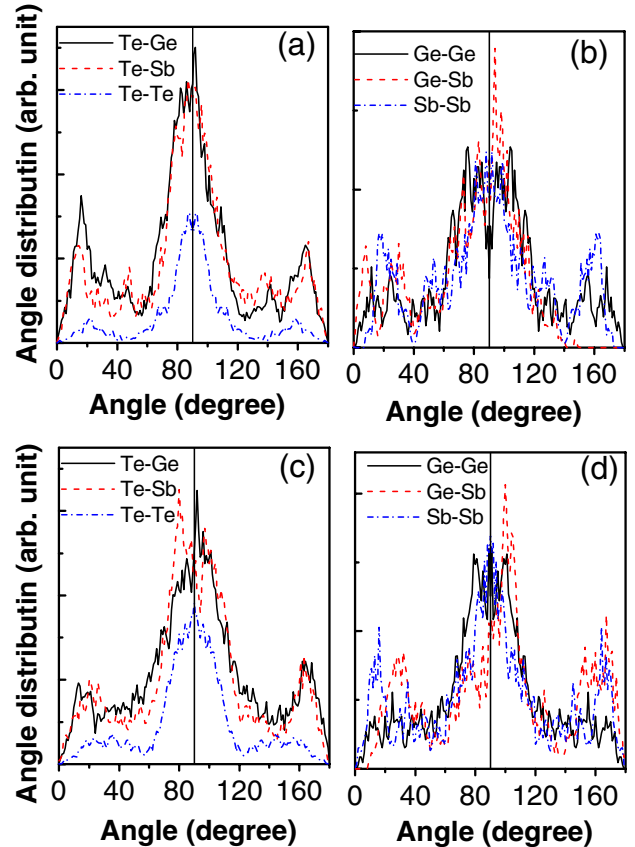


FIG. 4 (color online). Bond angle distributions for various pairs of bonds with respect to the $[111]$ crystallographic direction for $a1$ -GST (a) and (b), and for $a2$ -GST (c) and (d). The vertical lines show the corresponding angle positions for the Te-Te, Ge-Ge, and Sb-Sb bonds in c -GST.

configuration around Te atoms in *a*-GST is closest to its cubic form but showing the lowest chemical order. Therefore, the reversible phase transition between amorphous and cubic GST will involve the movement of Ge and Sb in contrast to the large displacement of Ge proposed by Kolobov [8].

It is clear now that pressure has a negligible effect on the topology around Ge and Sb in *a*-GST, but has a significant effect on the CSRO of Te and the arrangement of vacancies, while small effects of pressure on the configuration around Te is observed. Based on the above analysis, we suggest that both vacancies and Te play an important role in the fast reversible phase transition process. The large voids provide space for the rearrangement of atoms during phase transition. Therefore, it would be helpful to consider this effect when searching new phase-change memory materials and to improve the performance of Ge-Sb-Te alloys. Furthermore, we anticipate that the phenomenon of formation of large voids in molten and amorphous GST will be helpful to the study of defected amorphous systems.

Z. M. Sun and J. Zhou acknowledge support from the Natural Science Foundation of Fujian Province of China (No. 2008J0166) and Xiamen University.

*Author to whom correspondence should be addressed.

zmsun@xmu.edu.cn

zhmsun2@yahoo.com

- [1] N. Yamada, MRS Bull. **21**, 48 (1996).
[2] M. Chen, K. A. Rubin, and R. W. Barton, Appl. Phys. Lett. **49**, 502 (1986).

- [3] M. H. R. Lankhorst, B. W. S. M. M. Ketelaars, and R. A. M. Wolters, Nature Mater. **4**, 347 (2005).
[4] H. F. Hamann, M. O'Boyle, Y. C. Martin, M. Rooks, and H. K. Wickramasinghe, Nature Mater. **5**, 383 (2006).
[5] M. Wuttig and N. Yamada, Nature Mater. **6**, 824 (2007).
[6] M. Wuttig, D. Lüsebrink, D. Wamwangi, W. Weñic, M. Gillessen, and D. Dronskowski, Nature Mater. **6**, 122 (2007).
[7] S. R. Ovshinsky, Phys. Rev. Lett. **21**, 1450 (1968).
[8] A. V. Kolobov, P. Fons, A. I. Frenkel, A. L. Ankudinov, J. Tominaga, and T. Uruga, Nature Mater. **3**, 703 (2004).
[9] D. A. Baker, M. A. Paesler, G. Lucovsky, S. C. Agarwal, and P. C. Taylor, Phys. Rev. Lett. **96**, 255501 (2006).
[10] S. Kohara *et al.*, Appl. Phys. Lett. **89**, 201910 (2006).
[11] W. Weñic, A. Pamungkas, R. Detemple, C. Steimer, S. Blügel, and M. Wuttig, Nature Mater. **5**, 56 (2006).
[12] C. Bichara, M. Johnson, and J. P. Gaspard, Phys. Rev. **B75**, 060201(R) (2007).
[13] Z. Sun, J. Zhou, and R. Ahuja, Phys. Rev. Lett. **98**, 055505 (2007).
[14] Z. Sun, J. Zhou, and R. Ahuja, Phys. Rev. Lett. **96**, 055507 (2006).
[15] G. Kresse and J. Hafner, Phys. Rev. B **47**, 558 (1993).
[16] Z. M. Sun, J. Zhou, A. Blomqvist, B. Johansson, and R. Ahuja, Appl. Phys. Lett. **93**, 061913 (2008).
[17] W. K. Njoroge, H. W. Wöltgens, and M. Wuttig, J. Vac. Sci. Technol. A **20**, 230 (2002).
[18] D. M. Bylander and L. Kleinman, Phys. Rev. B **46**, 13 756 (1992).
[19] Z. M. Sun, J. Zhou, A. Blomqvist, L. H. Xu, and R. Ahuja, J. Phys. Condens. Matter **20**, 205102 (2008).
[20] M. Maret, P. Chieux, P. Hicter, M. Atzmon, and W. L. Johnson, J. Phys. F **17**, 315 (1987).